Version October 15, 2023
Preprint typeset using LaTeX style openjournal v. 09/06/15

PULSATION IN HOT MAIN SEQUENCE STARS: COMPARISON OF OBSERVATIONS WITH MODELS

L. A. Balona
South African Astronomical Observatory, P.O. Box 9, Observatory 7935, Cape Town, South Africa
Version October 15, 2023

ABSTRACT

TESS observations of pulsating hot main sequence stars paint a very different picture from what is currently accepted. There are large numbers of δ Scuti (DSCT) stars hotter than the theoretical hot edge of the instability strip, continuing to what appear to be DSCT stars of mid-B type (historically known as Maia variables). The frequencies of maximum amplitude in DSCT stars are in poor agreement with unstable frequencies from the models. There is a well-defined upper envelope in the frequencies of maximum amplitude as a function of effective temperature for DSCT and MAIA stars which requires an explanation. The γ Doradus (GDOR) stars should be regarded as DSCT stars with suppressed high frequencies rather than a separate class. They are found mostly among the cool DSCT stars, but occur throughout the DSCT instability strip and as early A-type stars, where they merge with the SPB variables. The mixture of DSCT and GDOR stars throughout the instability strip is one example of the unexplained large variation of frequency patterns in DSCT stars. The location of β Cephei stars in the H–R diagram agrees quite well with the models, but the observed frequencies are generally higher than predicted. There are no discernible boundaries between the traditional classes of pulsating stars. Existing pulsation models do not describe the observations at all well and a re-evaluation is required.

Subject headings: stars: oscillations — stars: early-type – stars: variables: general — stars: δ Scuti

1. INTRODUCTION

Prior to space observations, stellar pulsation among hot main sequence stars appeared to be well understood. The δ Scuti (DSCT) variables are F5–A2 dwarfs or giants with frequencies 5–50 d^{-1} in which pulsational driving is mostly attributed to the opacity κ mechanism operating in the He II partial ionization zone. For the cooler DSCT stars, coupling between convection and pulsation is important (Dupret et al. 2005; Xiong et al. 2016) and affords an explanation for the γ Doradus (GDOR) variables. These are stars with pulsation frequencies less than 5 d^{-1} lying on the cool edge of the DSCT instability strip.

The β Cephei (BCEP) variables, which are B4–O9 main sequence stars pulsating with frequencies in the range 3–20 d^{-1}, are driven by the opacity mechanism operating in the partial ionization zone of iron-like metals. The same mechanism is responsible for the SPB stars which have frequencies less than 3 d^{-1}. In these less massive stars, the iron opacity bump is located in a deeper layer. Together with the lower luminosity, this leads to an increase in the thermal timescale and lower pulsation frequencies. These SPB stars partially overlap the BCEP variables and extend to spectral type B8. Between the cool edge of the SPB variables and the hot edge of the DSCT stars, models do not predict pulsation.

Photometric time-series observations from space missions such as *CoRoT, Kepler* and *TESS* have increasingly challenged the above perceptions. From *CoRoT* observations, Degroote et al. (2009) reported low-amplitude late B-type pulsators lying between the SPB and DSCT instability strips with frequencies similar to those in DSCT stars. Such "Maia" variables, as they have historically been called, had been suspected from ground-based photometry (McNamara 1985; Lehmann et al. 1995; Percy & Wilson 2000; Kallinger et al. 2004). The existence of MAIA variables is now well established, not only from *Kepler* and *TESS* missions, but also from *Gaia* photometry (Gaia Collaboration et al. 2023).

Gravito-inertial modes have been detected in a number of stars (Pápics et al. 2012; Van Reeth et al. 2018; Mombarg et al. 2019; Ouazzani et al. 2020). These seem to be present, together with acoustic gravity modes, in GDOR stars. They arise in rotating stars where the Coriolis force acts as a restoring force. Rossby waves are seen as broad features in the periodograms of some DSCT variables (Saio et al. 2018). Mirouh (2022) has presented an excellent review of the various types of oscillations which may be present in rotating stars.

The general view, is that MAIA variables do not constitute a new group of pulsating stars. The high frequencies are presumed to be gravito-inertial modes shifted to high frequencies in rapidly-rotating SPB stars (Salmon et al. 2014). However, an analysis of their projected rotational velocities shows that this is not the case. In fact, over 10 % of MAIA variables have frequencies exceeding 60 d^{-1}. The MAIA variables appear to be an extension of the DSCT variables to early B stars (Balona 2023a).

Another factor challenging the accepted picture of pulsation among hot main sequence stars is that the GDOR variables are not confined to the instability region predicted by the models. GDOR stars are to be found all along the main sequence where they join up with the SPB stars (Balona et al. 2016). Models do not predict low frequencies for main sequence stars for effective temperatures in the range $7500 < T_{\rm eff} < 11,000$ K. Whether or not pulsation in these hot GDOR stars may be attributed to inertial modes is an open question. Another problem is the presence of low frequencies in DSCT stars hotter than about 7500 K. Grigahcène et al. (2010) found that DSCT stars with low frequencies (then called DSCT+GDOR "hybrids") exist all over the DSCT instability strip.

It turns out that there are no clear boundaries between any of the several types of hot pulsating stars

email: lab@saao.ac.za

GDOR, DSCT, MAIA, SPB and BCEP (Balona & Ozuyar 2020). This complicates the definition of the variability classes because arbitrary boundaries in effective temperature and frequency need to be introduced to uniquely define each variability class.

A very strange aspect is the huge variety of frequency patterns to be found in DSCT stars with similar effective temperatures, luminosities and rotation rates (Balona 2023b). It is self evident that stars with similar parameters should pulsate with similar frequencies and amplitudes, as models predict. This appears not to be the case. Each DSCT star somehow is able to modify the mode selection process to produce a unique frequency pattern which serves as a fingerprint for that star.

It seems that current perceptions of stellar pulsation in hot main sequence stars, which were adequate to explain ground-based observations, are no longer sufficient. The aim of this paper is to compare the predicted location of pulsation instability and the frequencies with *TESS* observations of hot main sequence stars. In this way, one might obtain clues as to how the models could be modified to better agree with observations. This work is based on a catalogue of the variability classes of over 125 000 *Kepler* and *TESS* stars on the upper main sequence compiled by Balona (2022) which is freely available.

2. THE DATA AND VARIABILITY CLASSIFICATION

The light curves obtained from the *Kepler* and *TESS* missions were used to construct periodograms. By inspecting the light curves and periodograms and knowing the approximate location of a star in the H–R diagram from its effective temperature or spectral type, a variability class can be assigned. This procedure was applied to about 125,000 stars observed by *Kepler* and *TESS*, mainly for stars brighter than 12.5 mag and hotter than 6000 K (Balona 2022). The catalogue is continuously updated, so the results described here include *TESS* sector 68.

The DSCT stars are defined to be main sequence F or A stars ($6000 < T_{\rm eff} < 10,000$ K) which pulsate with high frequencies. In this respect, "high frequency" is taken to mean any frequency higher than $5\,{\rm d}^{-1}$. Lower frequencies may, or may not, be present. If only frequencies less than $5\,{\rm d}^{-1}$ are present, the star is classified as GDOR.

Stars with frequencies less than $5\,{\rm d}^{-1}$ and in the temperature range $10,000 < T_{\rm eff} < 18,000$ K are classified as SPB. SPB variables also include stars with $T_{\rm eff} > 18,000$ K, but in this temperature range the maximum frequency is restricted to less than $3\,{\rm d}^{-1}$. This is necessary because BCEP stars may have frequencies as low as $3\,{\rm d}^{-1}$. Stars with $T_{\rm eff} > 18\,000$ K and at least one frequency peak higher than $3\,{\rm d}^{-1}$ are defined as BCEP. BCEP stars with low frequencies are classified as BCEP+SPB hybrids, but this may not be necessary as most BCEP stars are "hybrids" anyway.

Apart from the established classes described above, the MAIA class has been introduced. This is defined as any main sequence star with $10,000 < T_{\rm eff} < 18,000$ K and frequencies higher than $5\,{\rm d}^{-1}$. It is not possible to distinguish between MAIA and DSCT stars without introducing a temperature boundary. The value of $T_{\rm eff} = 10,000$ K was selected because it forms the boundary between the A- and B-type stars.

3. LOCATION IN THE H–R DIAGRAM

Evolutionary stellar models were computed using the Warsaw - New Jersey evolution code (Paczyński 1970), assuming an initial hydrogen fraction, $X_0 = 0.70$ and metal abundance, $Z = 0.020$ and using the chemical element mixture of Asplund et al. (2009) and OPAL opacities (Rogers & Iglesias 1992) Overshooting from the convective core was not included. A mixing length parameter $\alpha_{\rm MLT} = 1.0$ was adopted for the convective scale height. All models are non-rotating. The non-adiabatic code developed by Dziembowski (1977) was used to obtain the pulsation frequencies and growth rates. These models will be called the "Dziembowski" models.

Comparison of the location and extent of the observed and predicted instability strips is an important test of the models. With the above definitions, the observational instability strips for various classes are shown on the left panels of Fig. 1. This is to be compared with the unstable Dziembowski modes in the right panels of Fig. 1. The top panel shows stars with frequency peaks exceeding $5\,{\rm d}^{-1}$ (DSCT and MAIA) or exceeding $3\,{\rm d}^{-1}$ (BCEP), while the bottom panel shows the SPB and GDOR stars. Similarly, the figures on the right are divided into models with mostly p modes (top panel) or mostly g modes (bottom panel).

Also shown are the instability regions of the BCEP and SPB stars calculated by Miglio et al. (2007b). As can be seen on the right panels of Fig. 1, these agree rather well with the Dziembowski models. The agreement with observations (left panels) are also satisfactory. Also shown are the hot and cool edges of the DSCT and GDOR instability strips from Dupret et al. (2005) and Xiong et al. (2016). The agreement here is rather poor, particularly for models representing GDOR stars. None of the models represent the observations of DSCT stars at all well, but this depends on how the boundary between DSCT and MAIA stars is defined.

None of the models are able to reproduce MAIA stars nor the large number of SPB/GDOR stars between the cool edge of the SPB variables and the hot edge of the GDOR stars. In general, the major groups, DSCT and BCEP, can be understood as pulsational instability due to the opacity mechanisms acting in the ionization zones of He II and iron-group metals respectively. However, nothing else is readily understood in terms of the standard hypothesis of pulsational driving by the κ mechanism.

The number density of stars decreases rapidly with effective temperature. Whereas F0 stars are very common, B0 stars are very rare. Fig. 1 therefore gives a somewhat biased view of the relative number of stars of different variability classes. The fraction of stars of a given variability class relative to the number of main sequence stars at a particular temperature is shown in Fig, 2.

Over 500 MAIA variables have been classified from *TESS* photometry. The figure shows that MAIA variables comprise more than 10 % of mid- to late-B stars and are relatively more numerous than GDOR stars. The figure also shows that the large majority of main sequence stars do not seem to pulsate at all, or at least do not pulsate with amplitudes which can be detected by *TESS*. This, too, is not understood.

Fig. 2 again shows that the theoretical hot edge of

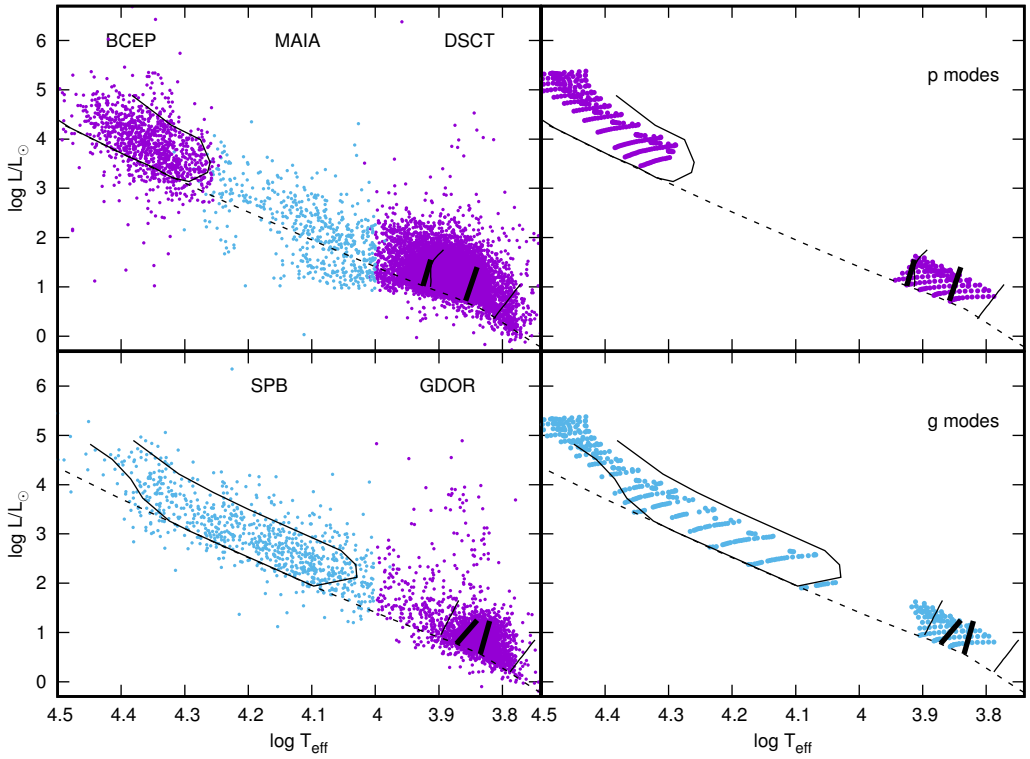

FIG. 1.— The location of various classes of pulsating stars in the H–R diagram (left panels) and location of Dziembowski models showing unstable p and g modes (right panels). The dashed line is the zero-age main sequence. Also shown are the instability regions in BCEP and SPB stars for solar abundance models by Miglio et al. (2007a) and the hot and cool edges of the DSCT and GDOR stars from Dupret et al. (2005) (thick lines) and Xiong et al. (2016) (thin lines).

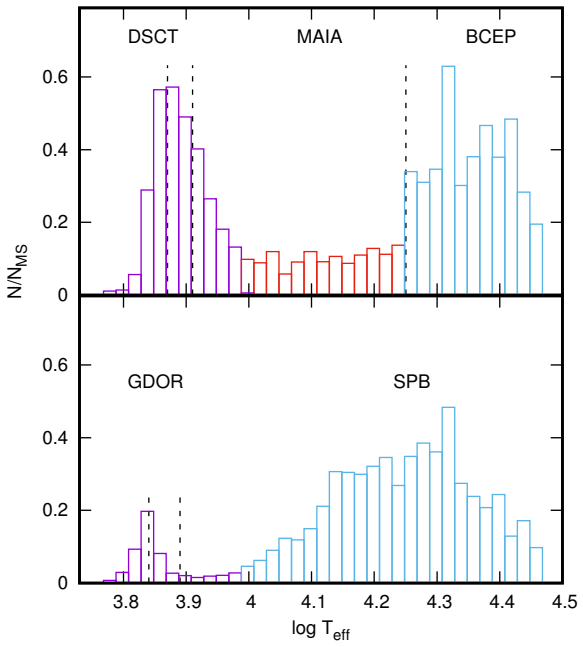

FIG. 2.— The ratio $N/N_{\rm MS}$ as a function of effective temperature. N is the number of stars of the particular variability class and $N_{\rm MS}$ is the number of main sequence stars within the temperature bin size. The vertical dashed lines indicate the minimum and maximum temperature of the hot edge of DSCT and GDOR stars predicted by various models. The cool edge of the BCEP instability region from Miglio et al. (2007b) is shown.

DSCT stars does not agree with observations. It can also be seen that the relative numbers of DSCT stars match smoothly with that of MAIA variables. The MAIA stars could just as well be considered as an extension of the DSCT variables.

4. PULSATION FREQUENCIES

In the previous section it was shown that pulsation models fail to correctly predict the hot edge of the DSCT instability region, the MAIA stars or the large number of low-frequency pulsators between the SPB and GDOR instability strips. In this section, the frequencies of unstable modes from models are compared to the observed frequencies.

In the top panel of Fig. 3, the frequency of largest amplitude, ν_1, is shown as a function of effective temperature. This may be compared with the frequencies of unstable modes with $l \leq 2$ in non-rotating Dziembowski models (middle panel). The difference between the observed and predicted frequencies for GDOR stars is understandable, because the adoption of frozen-in convection in the models is not very satisfactory. This should not affect models of the hotter stars where convection may perhaps be less important. The Dziembowski models also predict a lack of low frequencies for DSCT stars with $\log T_{\rm eff} > 3.87$, in contradiction with observations.

Some of the discrepancies between the observed and predicted frequencies may be attributed to rotation. Rotation not only introduces additional modes, but also tends to reduce the frequencies given by non-rotating models. These effects can be crudely simulated by apply-

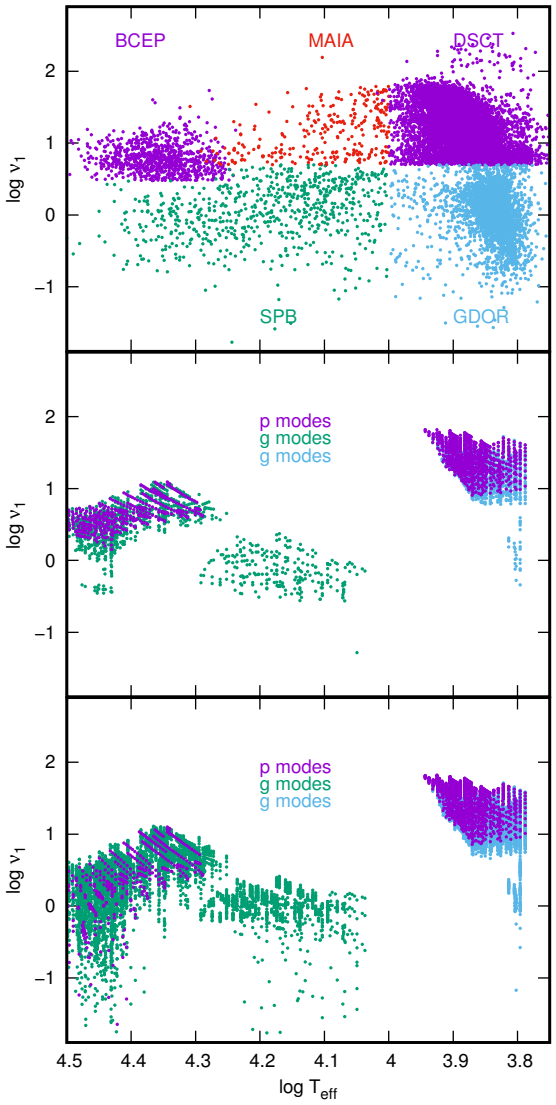

FIG. 3.— The top panel shows the frequency of largest amplitude of various types of *TESS* pulsating stars as a function of effective temperature. The middle panel shows the frequencies of unstable modes with $l \leq 2$ in non-rotating Dziembowski models. In the bottom panel, the model frequencies are modified by applying a rotation rate of $1\,\mathrm{d}^{-1}$.

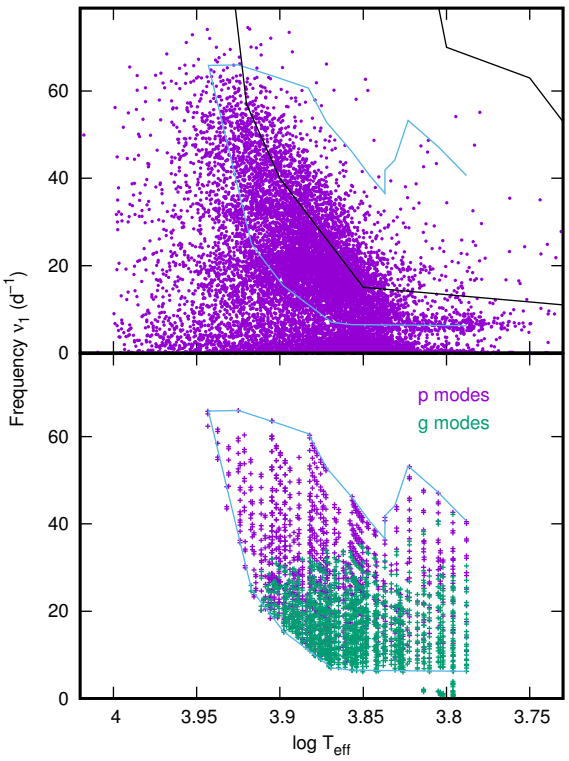

FIG. 4.— The top panel shows the frequency of maximum amplitude as a function of effective temperature for DSCT stars. The black outline is the envelope of the highest amplitude growth rate of low-degree p modes shown in Fig. 9 of Xiong et al. (2016). The blue outline is the envelope of unstable modes from Dziembowski models. The frequencies of unstable modes in the Dziembowski models is shown in the bottom panel.

ing the third-order rotational perturbation formula given in Reese et al. (2006) to the non-rotating model frequencies. Modes with spherical harmonic degree l are split into $2l+1$ components of equal amplitude. A constant rotation rate of $1\,\mathrm{d}^{-1}$ was applied, but gravitational darkening at the equator was ignored.

The result (bottom panel of Fig. 3), shows that the mixed p- and g-modes in BCEP stars are moved by rotation to frequencies typical of SPB stars. This reduces the frequency gap between the BCEP and SPB stars, in closer agreement with observations.

The top panel of Fig. 3 shows a surprisingly well-defined upper frequency envelope in DSCT stars. The frequency of maximum amplitude, ν_1, increases with temperature, reaching a maximum at about $\log T_{\rm eff} \approx 3.93$ before decreasing. The decrease in ν_1 continues in the MAIA stars. This is shown in more detail for the DSCT stars in the top panel of Fig. 4. The bottom panel shows unstable p and g modes from the Dziembowski models. The schematic envelope in this figure is reproduced in the top panel (blue line). Also shown in the top panel is the schematic envelope of p-mode frequencies with the highest growth rate from Fig. 9 of Xiong et al. (2016) (black line).

The frequencies of DSCT stars derived by Xiong et al. (2016) are in very poor agreement with observations. The frequencies from the Dziembowski models are in somewhat better agreement, but far from satisfactory. For $\log T_{\rm eff} > 3.87$, low frequencies are stable in the Dziembowski models, whereas observations show that DSCT stars with low frequencies are the rule rather than the exception.

It does not matter whether the frequency of largest amplitude, ν_1, or second-largest amplitude, ν_2 or, indeed, the frequency with the n-th largest amplitude, ν_n, is used. The upper envelope of frequency as a function of effective temperature is always quite sharp. There is no obvious reason why such a well-defined frequency envelope should exist. The frequency of the envelope increases slowly with n.

If, instead, the maximum frequency, $\nu_{\rm max}$, is plotted as a function of effective temperature, the result is similar to Fig. 4, except that the envelope is shifted towards higher frequencies by about 20 %. This is still considerably lower than the estimated critical frequency, which is the frequency beyond which the pulsational acoustic waves are no longer reflected in the atmosphere.

5. IS THE GDOR CLASS NECESSARY?

The frequency threshold of $\nu_t = 5\,\mathrm{d}^{-1}$, used to distinguish between DSCT and GDOR stars, has no basis in theory. It was adopted because frequencies lower than $5\,\mathrm{d}^{-1}$ were never seen in ground-based photometry of DSCT stars. This is not surprising because variations in atmospheric extinction and low pulsation amplitudes makes the detection of low frequencies very difficult from ground-based photometry. It is possible that there is no real difference between DSCT and GDOR stars.

The detection of multiple low frequency peaks in GDOR stars was unexpected and not predicted from the pulsation models available at that time. For this reason, it was presumed to be a new class of pulsating variable (Balona et al. 1994). Many more GDOR stars were subsequently discovered (Henry et al. 2007). However, there was no similar attempt to detect low frequencies in the DSCT stars known at the time.

The first example of "hybrid" DSCT+GDOR pulsation was discovered by (Handler et al. 2002). Until the advent of space photometry, only 6 hybrids and 66 GDOR stars were known. Surprisingly, the first *Kepler* release revealed that most DSCT stars were actually hybrids (Grigahcène et al. 2010). Indeed, among the *TESS* DSCT stars, about 75 % are hybrids.

In retrospect, it seems that if sufficient photometric precision were available, ground-based observations would have detected low frequencies in most DSCT stars at an early stage. In that case, the definition of DSCT stars would not have excluded low frequencies. What we now call GDOR stars would not have been a surprise and most likely regarded simply as DSCT stars with low frequencies.

Guzik et al. (2000) were able to model low frequencies by proposing the convective blocking mechanism. Later, Dupret et al. (2005) and Xiong et al. (2016) were able to show that the low frequencies could be modeled using a time-dependent convection theory. Xiong et al. (2016), in fact, found that there is no essential difference between DSCT and GDOR stars. They can be considered as just two subgroups of one broader variability class.

Since there seems no need to differentiate between DSCT and GDOR stars in the models, it seems appropriate to re-evaluate the relevance of a separate GDOR class. Fig. 5 shows the DSCT and GDOR stars in the H–R diagram. For convenience, the boundary of the DSCT and GDOR stars is approximated by a trapezoid (green) and triangle (orange) respectively. Most GDOR stars are located inside the triangular region on the cool side of the DSCT stars, more or less within the region of low-frequency g-mode instability predicted by Xiong et al. (2016). The models by Dupret et al. (2005) predict a much smaller region.

There are 3995 DSCT stars and 3237 GDOR stars inside the triangular GDOR region. In other words, there are as many DSCT stars as GDOR stars. The presence of GDOR and DSCT stars occupying the same region of the H–R diagram is clearly impossible to duplicate in pulsation models. Furthermore, there is a large number of GDOR stars outside the main triangular region, extending well beyond the hot edge of DSCT stars. This, too, cannot be explained by current models. Furthermore, there are 35,792 *TESS* main sequence stars within the triangular γ Dor region that are not observed to pulsate at all. The presence of stars with high frequencies, stars with low frequencies and ostensibly non-pulsating stars in the same region of the H–R diagram is not understood. Models predict that all stars should pulsate.

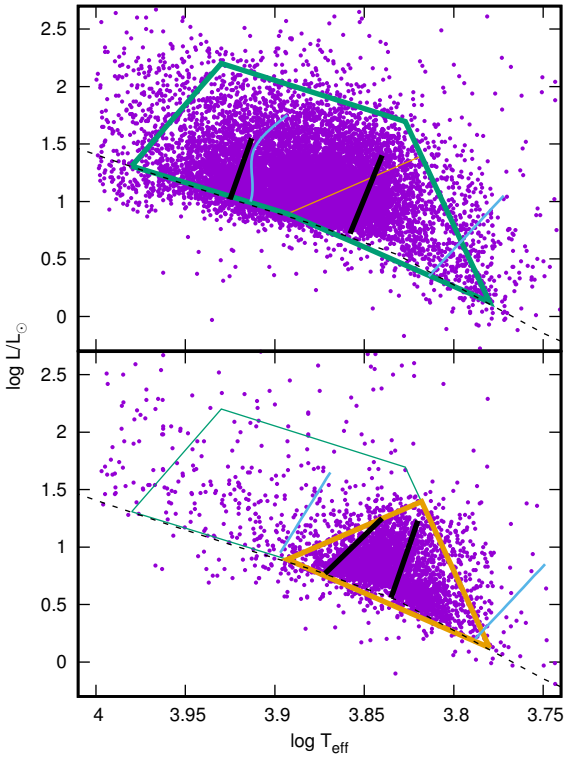

FIG. 5.— The top panel shows the location of 12772 *TESS* DSCT stars in the H–R diagram enclosed by a schematic trapezium (green). The hot and cool edges from Dupret et al. (2005) (thick black lines) and Xiong et al. (2016) (thin blue lines). The bottom panel shows 4065 *TESS* GDOR stars enclosed by schematic triangle (orange) and corresponding hot and cool edges. The diagonal dashed line is the zero-age main sequence.

Suppose that a threshold frequency, ν_t, is used to discriminate between GDOR and DSCT stars. Let n be the number of significant frequency peaks below ν_t. If there is any significance to ν_t, then one might hope to detect a difference in the distribution of n as a function of ν_t. When this procedure is carried out with $\nu_t = 4, 6, 8, 10\,\mathrm{d}^{-1}$, it is found that the distributions of n are very similar. This suggests that there is no reason to regard stars with low frequencies any differently from normal DSCT stars. However, it is necessary to understand why stars with low frequencies are predominantly located in the triangular region.

6. CONNECTION BETWEEN DSCT AND MAIA

It is evident from Fig. 5 that the theoretical hot edge of the DSCT instability strip does not agree with observations. There are a great number of DSCT stars hotter than the predicted hot edge continuing well past $T_{\mathrm{eff}} = 10,000\,\mathrm{K}$ where they merge with the MAIA variables.

Balona (2023a) has shown that there is no difference in rotation rate between MAIA stars and normal main sequence stars and that the amplitude distribution of MAIA variables is the same as in DSCT stars, but dif-

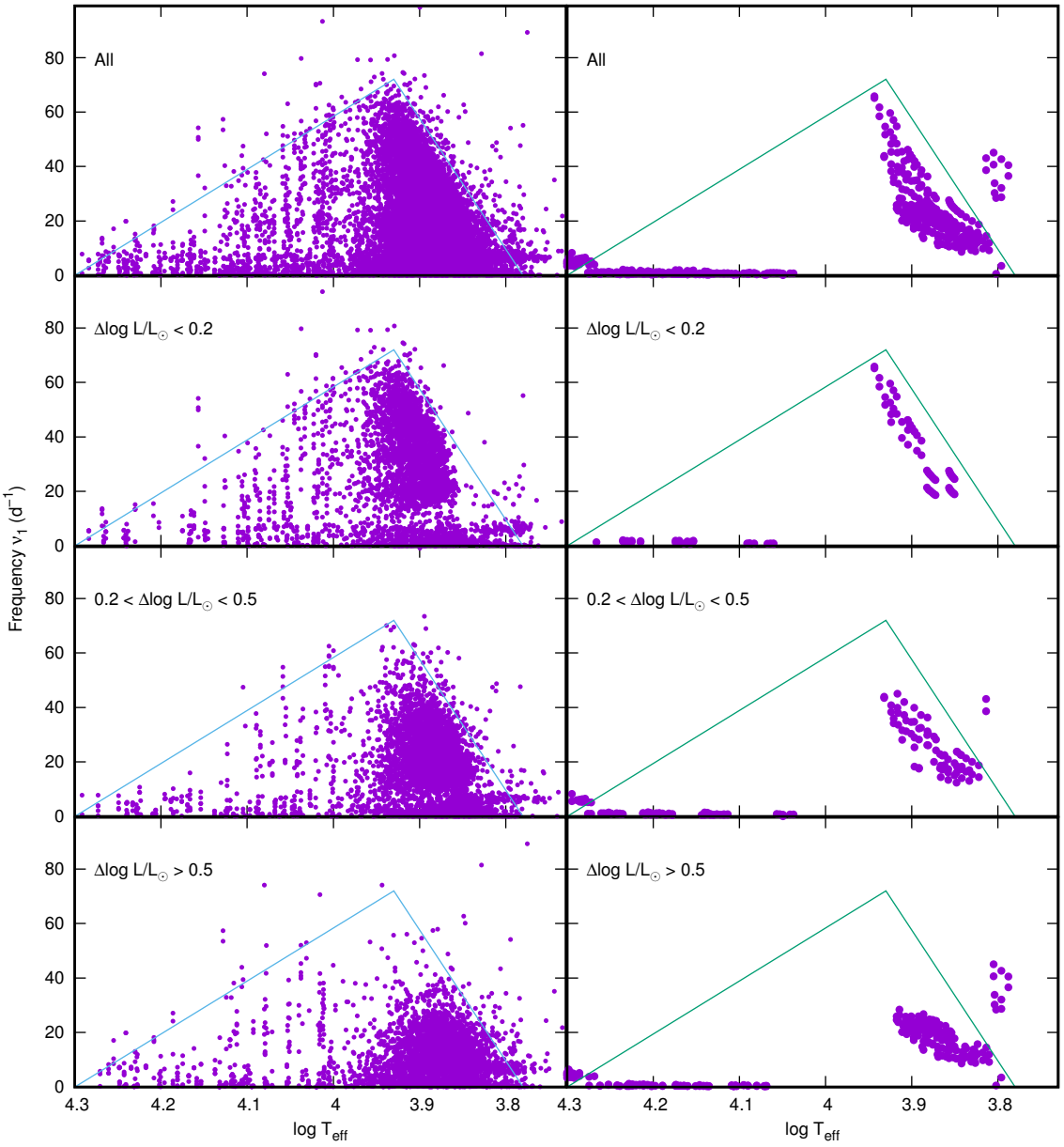

FIG. 6.— The frequency of maximum amplitude as a function of effective temperature. The top left panel shows all DSCT and MAIA stars enclosed by a schematic triangular envelope. The other panels on the left show stars selected according to $\Delta L/L_\odot$, the luminosity above the zero-age main sequence. The panels on the right are the corresponding frequencies from the Dziembowski models.

ferent from BCEP stars. One may as well regard MAIA stars as an extension of DSCT variables to hotter temperatures, but this should await a theory of unstable high-frequency modes in late- to early-B stars.

The left panels of Fig. 6 show ν_1, the frequency of maximum amplitude, as a function of effective temperature for DSCT and MAIA stars. For MAIA stars, the plot actually shows ν_5, the frequencies of the five highest amplitude peaks. This is to balance the large difference in number density between the two classes.

The top left panel of Fig. 6 shows that there is a roughly linear increase in ν_1 from the coolest DSCT stars, reaching a maximum of about $72\,\mathrm{d}^{-1}$ at $\log T_{\rm eff} \approx 3.93$. Thereafter the frequency decreases with temperature, reaching a minimum at the hot end of the MAIA variables, as shown by the blue lines in the figure. The systematic decrease in ν_1 initiated in the hot DSCT stars and continued by the MAIA variables seems to be another link between DSCT and MAIA stars.

The top right panel of Fig. 6 shows the frequencies ν_2, of the first two unstable modes of highest amplitude as a function of temperature. Since the Dziembowski models do not actually calculate the amplitudes, these are taken to be proportional to the growth rate and mode visibility. Not surprisingly, nearly all the modes in this plot are radial with radial order increasing with frequency from 1 to 8. The increase in frequency with increasing temperature is also visible in the models.

Fig. 6 also shows the ν_1–$\log T_{\rm eff}$ diagram for stars in different luminosity ranges, $\Delta L/L_\odot$, above the zero-age main sequence (ZAMS). As $\Delta L/L_\odot$ increases, the frequency of maximum amplitude decreases from $72\,\mathrm{d}^{-1}$

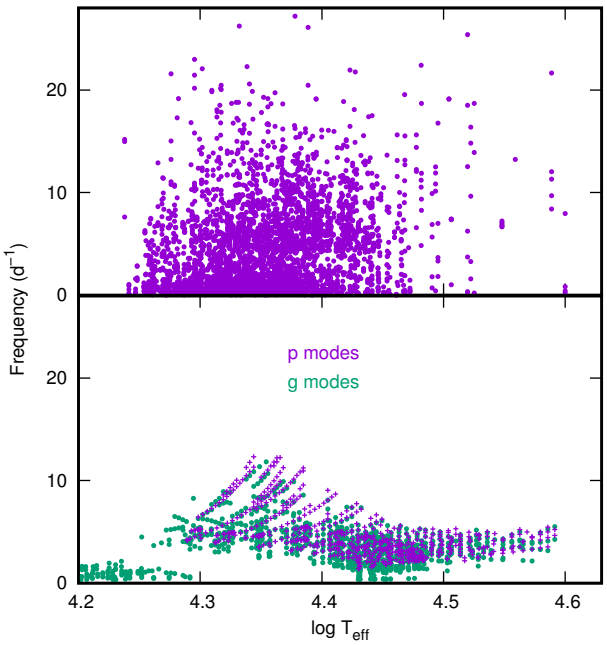

FIG. 7.— All observed frequencies in BCEP, BCEP+SPB or pure SPB stars in the BCEP temperature range are shown in the top panel. The bottom panel shows unstable modes for $l \leq 2$ from Diembowski models.

near the ZAMS to about $40\,\mathrm{d}^{-1}$ for the most evolved stars. The corresponding effective temperature at maximum frequency decreases from 8500 K for stars close to the ZAMS, to about 7500 K for more evolved stars. A similar behaviour seems to be present in the Dziembowski models (right panels in the figure).

The relationship between effective temperature and frequency in DSCT stars has been investigated by many authors. Barceló Forteza et al. (2018, 2020) found a linear relationship between an amplitude-weighted frequency and $T_{\rm eff}$ in DSCT stars. Bowman & Kurtz (2018) found a similar relationship for the frequency of maximum amplitude. However, as can be seen from the above figures, there is no unique relationship between ν_1 and $\log T_{\rm eff}$.

7. THE SPB AND BCEP STARS

Unless colours in the U band are available, it is not possible to distinguish between the effect of temperature and interstellar reddening for B stars. Since modern CCDs are not sensitive in the U band, one has to rely mostly on spectroscopic estimates of effective temperature or estimates from Strömgren or Geneva photometry. The proportion of B stars with reliable effective temperatures is therefore considerably smaller than in A or F stars. The spectral type and luminosity class often provides the only reliable estimate of $T_{\rm eff}$ for B stars.

The defined lower bound in effective temperature for SPB stars, $T_{\rm eff} = 10,000$ K, is less than the cool edge derived from models of non-rotating SPB stars by about 1000 K. It has been shown that SPB stars cooler than the theoretical cool edge do not rotate at a significantly higher rate than normal main sequence stars (Balona 2023a). Rapid rotation cannot therefore be used to explain the presence of SPB stars beyond the cool edge. Stars with frequencies typical of SPB or GDOR stars occur all along the main sequence. Models fail to reproduce this continuous sequence of low-frequency pulsators.

In the catalog of Stankov & Handler (2005), there are 93 confirmed BCEP variables. An additional 103 BCEP stars are found in the photometric survey by Pigulski & Pojmański (2008). To these can be added the 86 new BCEP variables discovered by Labadie-Bartz et al. (2020), for a total of 282 known BCEP stars. In Balona (2022), 800 new BCEP stars have been detected, bringing the total to 1082 BCEP stars identified from *TESS* photometry. Of these, 621 are classified as BCEP+SPB hybrids.

Since 57 % of BCEP stars are classified as BCEP+SPB, the question arises as to whether the presence of low frequencies can be considered a normal occurrence. In that case, as in the case of the DSCT+GDOR hybrids, one may abandon the designation BCEP+SPB and refer to BCEP stars with low frequencies simply as BCEP.

The problem with BCEP+SPB hybrids is not merely a problem of classification. According to models, BCEP stars should not pulsate with frequencies lower than about $3\,\mathrm{d}^{-1}$. This is because g modes have high amplitudes in the core and are heavily damped. The structure of the eigenfunction does play a role and, for some modes, driving can exceed damping in the inner layers. To model the low frequencies requires an increase in opacity by about a factor of four (Pamyatnykh et al. 2004).

The problem can be seen in the middle panel of Fig. 3 or the bottom panel of Fig. 7. There is a distinct frequency gap between non-rotating models of SPB stars and BCEP stars, whereas no such gap appears in the observations. There are no unstable frequencies less than $3\,\mathrm{d}^{-1}$ for BCEP stars cooler than $\log T_{\rm eff} \approx 4.40$. The discrepancy between the models and observations may be reduced, to some extent, by a choice of OP opacities rather than OPAL opacities (Dziembowski & Pamyatnykh 2008; Miglio et al. 2007b).

In a BCEP star, mixed modes are moved to lower frequencies by rotation (bottom panel of Fig. 3). If rotation is the correct explantion for the BCEP hybrids, pure BCEP stars should rotate more slowly than than BCEP+SPB hybrids. From 123 pure BCEP stars $\langle v \sin i \rangle = 113 \pm 8\,\mathrm{km\,s}^{-1}$ and from 354 BCEP+SPB stars $\langle v \sin i \rangle = 158 \pm 6\,\mathrm{km\,s}^{-1}$. This seems to suggest that rotation could indeed be considered as possible explanation for the BCEP hybrids, but more evidence is required.

The top panel of Fig. 7 shows the complete set of frequencies observed in BCEP, BCEP+SPB and pure SPB stars in the BCEP temperature range as a function of effective temperature. The upper envelope is quite well defined, reaching a maximum frequency of about $18\,\mathrm{d}^{-1}$ at $T_{\rm eff} \approx 22,000$ K. However, frequencies in the non-rotating models (bottom panel) do not exceed $13\,\mathrm{d}^{-1}$. In spite of this discrepancy, BCEP stars show the best agreement with pulsation models.

8. TWO UNUSUAL BCEP STARS

There are two unusual B stars which qualify as BCEP, but have very high frequencies. TIC 119462263 (HD 133518) is a He-strong star (B2IVp) (Zboril & North 2000) with a strong magnetic field (Alecian et al. 2014). The pulsation frequencies are 57.391 and $54.169\,\mathrm{d}^{-1}$ with a possible third peak at $60.727\,\mathrm{d}^{-1}$. These frequencies are much higher than generally seen in BCEP stars. Al-

though the field is quite crowded, the star is very bright ($V = 6.4$ mag) and other stars within a 2 arcmin field of view are fainter than 10-th magnitude.

TIC 340410923 (HD 152407) is another interesting star. It has been classified as O8f? (Morgan et al. 1955) or B5Ib (Houk 1978). with a rich system of frequency peaks stretching up to $71.14\,\mathrm{d}^{-1}$. However, the Strömgren $\beta = 2.836$ (Paunzen 2015) suggests an early A star. Contamination from neighbouring stars is more of a problem. Both stars deserve further investigation.

9. CONCLUSIONS

In this paper, the observed regions of instability in the H–R diagram for various classes of pulsating star are compared with predictions from pulsation models. The frequencies of maximum amplitude are also compared with models. It is concluded that, except possibly for BCEP stars, the models do not agree at all well with observations.

One of the most serious problems is that DSCT stars do not behave as predicted at a very basic level. It is taken for granted that stars with the same effective temperature, luminosity and rotation rate should have the same frequencies. This is, of course, what models predict, but not what observations show. Balona (2023b) has shown that the frequency patterns in DSCT stars are very different for stars with approximately the same effective temperature and luminosity. Differing rotation rates and inclinations do not solve the problem. Each star has a unique fingerprint of frequencies and amplitudes. This suggests that mode selection may be a highly non-linear process determined by local conditions.

The presence of equal numbers of DSCT and GDOR in the same region of the H–R diagram shows that the GDOR and DSCT stars cannot be regarded as two separate classes. Rather, the GDOR stars should be considered in the light of the wide variety of frequency patterns just mentioned. In other words, GDOR stars should be regarded simply as DSCT stars in which high frequencies are suppressed.

The location of the hot edge of the DSCT instability strip in the models should be relatively accurate because the effect of convection is negligible, at least according to current understanding. The observations show, however, that DSCT stars hotter than the predicted hot edge are numerous. In fact, substantial numbers of DSCT stars are present not only among early A stars, but also among late to mid-B stars where they are called MAIA variables.

There are serious discrepancies between the observed frequencies and frequencies of unstable modes in models of DSCT stars. For example, the models of Xiong et al. (2016) predict frequencies which are far higher than observed. Frequencies from the Dziembowski models also do not agree well with observations. Frequencies of BCEP stars from the models are in reasonable agreement with observations, but lower than observed.

The multiple failures of pulsation models described above requires a re-assessment of the basic assumptions underlying the models. Perhaps there is more than one driving mechanism active in upper main sequence stars. This might explain why DSCT and MAIA variables are seen over a very wide range of effective temperature.

It is found that there is a well-defined envelope for the frequency of maximum amplitude as a function of temperature. This was unexpected and with no obvious explanation. The frequency and frequency range is smallest for the coolest DSCT stars and increases smoothly with temperature. The frequency reaches a maximum of about $72\,\mathrm{d}^{-1}$ at $T_{\rm eff} \approx 8500$ K then decreases smoothly. The decrease in frequency and frequency range with temperature continues with the MAIA variables, eventually reaching a minimum at about $T_{\rm eff} \approx 18,000$ K. This characteristic feature does not seem to have been noticed before. It may provide a clue to the nature of DSCT and MAIA stars.

ACKNOWLEDGMENTS

I wish to thank the National Research Foundation of South Africa for financial support.

DATA AVAILABILITY

The data underlying this article can be obtained from `https://sites.google.com/view/tessvariables/home`. and also available though the author.

REFERENCES

Alecian E., Kochukhov O., Petit V., et al., 2014, A&A, 567, A28
Asplund M., Grevesse N., Sauval A. J., Scott P., 2009, ARA&A, 47, 481
Balona L. A., 2022, arXiv e-prints, arXiv:2212.10776
—, 2023a, Frontiers in Astronomy and Space Sciences, 10, 1266750
—, 2023b, The Open Journal of Astrophysics, 6, 28
Balona L. A., Engelbrecht C. A., Joshi Y. C., et al., 2016, MNRAS, 460, 1318
Balona L. A., Krisciunas K., Cousins A. W. J., 1994, MNRAS, 270, 905
Balona L. A., Ozuyar D., 2020, MNRAS, 493, 5871
Barceló Forteza S., Moya A., Barrado D., Solano E., Martín-Ruiz S., Suárez J. C., García Hernández A., 2020, A&A, 638, A59
Barceló Forteza S., Roca Cortés T., García R. A., 2018, A&A, 614, A46
Bowman D. M., Kurtz D. W., 2018, MNRAS, 476, 3169
Degroote P., Aerts C., Ollivier M., et al., 2009, A&A, 506, 471
Dupret M., Grigahcène A., Garrido R., Gabriel M., Scuflaire R., 2005, A&A, 435, 927
Dziembowski W., 1977, Acta Astronomica, 27, 95
Dziembowski W. A., Pamyatnykh A. A., 2008, MNRAS, 385, 2061
Gaia Collaboration, De Ridder J., Ripepi V., et al., 2023, A&A, 674, A36
Grigahcène A., Antoci V., Balona L., et al., 2010, ApJ, 713, L192
Guzik J. A., Kaye A. B., Bradley P. A., Cox A. N., Neuforge C., 2000, ApJ, 542, L57
Handler G., Balona L. A., Shobbrook R. R., et al., 2002, MNRAS, 333, 262
Henry G. W., Fekel F. C., Henry S. M., 2007, AJ, 133, 1421
Houk N., 1978, Michigan catalogue of two-dimensional spectral types for the HD stars
Kallinger T., Iliev I., Lehmann H., Weiss W. W., 2004, in IAU Symposium, Vol. 224, The A-Star Puzzle, J. Zverko, J. Ziznovsky, S. J. Adelman, & W. W. Weiss, ed., pp. 848–852
Labadie-Bartz J., Handler G., Pepper J., Balona L. A., De Cat P., Stevens D. J., Lund M. B., et al., 2020, AJ, 160, 32
Lehmann H., Scholz G., Hildebrandt G., Klose S., Panov K. P., Reimann H.-G., Woche M., Ziener R., 1995, A&A, 300, 783
McNamara B. J., 1985, ApJ, 289, 213
Miglio A., Montalbán J., Dupret M., 2007a, Communications in Asteroseismology, 151, 48
Miglio A., Montalbán J., Dupret M.-A., 2007b, MNRAS, 375, L21
Mirouh G. M., 2022, Frontiers in Astronomy and Space Sciences, 9, 952296

Mombarg J. S. G., Van Reeth T., Pedersen M. G., Molenberghs G., Bowman D. M., Johnston C., Tkachenko A., Aerts C., 2019, MNRAS, 485, 3248
Morgan W. W., Code A. D., Whitford A. E., 1955, ApJS, 2, 41
Ouazzani R. M., Lignières F., Dupret M. A., Salmon S. J. A. J., Ballot J., Christophe S., Takata M., 2020, A&A, 640, A49
Paczyński B., 1970, Acta Astronomica, 20, 47
Pamyatnykh A. A., Handler G., Dziembowski W. A., 2004, MNRAS, 350, 1022
Pápics P. I., Briquet M., Baglin A., et al., 2012, A&A, 542, A55
Paunzen E., 2015, A&A, 580, A23
Percy J. R., Wilson J. B., 2000, PASP, 112, 846
Pigulski A., Pojmański G., 2008, A&A, 477, 917
Reese D., Lignières F., Rieutord M., 2006, A&A, 455, 621
Rogers F. J., Iglesias C. A., 1992, ApJS, 79, 507
Saio H., Kurtz D. W., Murphy S. J., Antoci V. L., Lee U., 2018, MNRAS, 474, 2774
Salmon S. J. A. J., Montalbán J., Reese D. R., Dupret M.-A., Eggenberger P., 2014, A&A, 569, A18
Stankov A., Handler G., 2005, ApJS, 158, 193
Van Reeth T., Mombarg J. S. G., Mathis S., et al., 2018, A&A, 618, A24
Xiong D. R., Deng L., Zhang C., Wang K., 2016, MNRAS, 457, 3163
Zboril M., North P., 2000, Contributions of the Astronomical Observatory Skalnate Pleso, 30, 12